

University of Wollongong

Research Online

---

Faculty of Engineering and Information  
Sciences - Papers: Part B

Faculty of Engineering and Information  
Sciences

---

2018

## Axial Load-Axial Deformation Behaviour of SCC Columns Reinforced with Steel Tubes

Faez Alhussainy

*University of Wollongong, fama867@uowmail.edu.au*

M Neaz Sheikh

*University of Wollongong, msheikh@uow.edu.au*

Muhammad N. S Hadi

*University of Wollongong, mhadi@uow.edu.au*

Follow this and additional works at: <https://ro.uow.edu.au/eispapers1>



Part of the [Engineering Commons](#), and the [Science and Technology Studies Commons](#)

---

### Recommended Citation

Alhussainy, Faez; Sheikh, M Neaz; and Hadi, Muhammad N. S, "Axial Load-Axial Deformation Behaviour of SCC Columns Reinforced with Steel Tubes" (2018). *Faculty of Engineering and Information Sciences - Papers: Part B*. 1739.

<https://ro.uow.edu.au/eispapers1/1739>

Research Online is the open access institutional repository for the University of Wollongong. For further information contact the UOW Library: [research-pubs@uow.edu.au](mailto:research-pubs@uow.edu.au)

---

# Axial Load-Axial Deformation Behaviour of SCC Columns Reinforced with Steel Tubes

## Abstract

A simplified analytical model has been developed for the axial load-axial deformation behaviour of self-compacting concrete (SCC) columns reinforced with steel tubes. The developed analytical model takes into account the contribution of the steel tubes, unconfined concrete cover, confined concrete core and confined concrete inside the steel tube. The results of the analytical model have been compared with experimental results of four SCC column specimens. The results of the analytical model are in good agreement with the experimental results. A parametric study has been conducted to investigate the influences of the compressive strength of SCC, tensile strength of steel tube, wall thickness of steel tube and pitch of steel helix on the axial load-axial deformation behaviour of SCC columns reinforced with steel tubes. The ductility of SCC columns has been found to be significantly influenced by the increase in the compressive strength of SCC and the pitch of steel helix.

## Disciplines

Engineering | Science and Technology Studies

## Publication Details

Alhussainy, F., Sheikh, M. Neaz. & Hadi, M. N. S. (2018). Axial Load-Axial Deformation Behaviour of SCC Columns Reinforced with Steel Tubes. *Structures*, 15 259-269.

Accepted Manuscript

Axial Load-Axial Deformation Behaviour of SCC Columns Reinforced with Steel Tubes

Faez Alhussainy, M. Neaz Sheikh, Muhammad N.S. Hadi



PII: S2352-0124(18)30070-5  
DOI: doi:[10.1016/j.istruc.2018.07.006](https://doi.org/10.1016/j.istruc.2018.07.006)  
Reference: ISTRUC 300  
To appear in: *Structures*  
Received date: 16 March 2018  
Revised date: 19 June 2018  
Accepted date: 15 July 2018

Please cite this article as: Faez Alhussainy, M. Neaz Sheikh, Muhammad N.S. Hadi , Axial Load-Axial Deformation Behaviour of SCC Columns Reinforced with Steel Tubes. *Istruc* (2018), doi:[10.1016/j.istruc.2018.07.006](https://doi.org/10.1016/j.istruc.2018.07.006)

This is a PDF file of an unedited manuscript that has been accepted for publication. As a service to our customers we are providing this early version of the manuscript. The manuscript will undergo copyediting, typesetting, and review of the resulting proof before it is published in its final form. Please note that during the production process errors may be discovered which could affect the content, and all legal disclaimers that apply to the journal pertain.

## Axial Load-Axial Deformation Behaviour of SCC Columns Reinforced with Steel Tubes

Faez Alhussainy<sup>1</sup>

<sup>1</sup> Ph.D. Candidate, School of Civil, Mining, and Environmental Engineering,  
University of Wollongong, Australia.

Email: [fama867@uowmail.edu.au](mailto:fama867@uowmail.edu.au)

M. Neaz Sheikh<sup>2</sup>

<sup>2</sup> Associate Professor, School of Civil, Mining, and Environmental Engineering,  
University of Wollongong, Australia.

Email: [msheikh@uow.edu.au](mailto:msheikh@uow.edu.au)

Muhammad N. S. Hadi<sup>3,\*</sup> (Fellow of ASCE)

<sup>3</sup> Associate Professor, School of Civil, Mining, and Environmental Engineering,  
University of Wollongong, Australia.

Email: [mhadi@uow.edu.au](mailto:mhadi@uow.edu.au),

\*Corresponding author

### Abstract

A simplified analytical model has been developed for the axial load-axial deformation behaviour of self-compacting concrete (SCC) columns reinforced with steel tubes. The developed analytical model takes into account the contribution of the steel tubes, unconfined concrete cover, confined concrete core and confined concrete inside the steel tube. The results of the analytical model have been compared with experimental results of four SCC column specimens. The results of the analytical model are in good agreement with the experimental results. A parametric study has been conducted to investigate the influences of the compressive strength of SCC, tensile strength of steel tube, wall thickness of steel tube and

pitch of steel helix on the axial load-axial deformation behaviour of SCC columns reinforced with steel tubes. The ductility of SCC columns has been found to be significantly influenced by the increase in the compressive strength of SCC and the pitch of steel helix.

**Keywords:** Composite columns; self-compacting concrete; steel tube; axial load-axial deformation; ductility.

## 1. Introduction

Steel sections and concrete are commonly used in the construction of composite columns. There are two main configurations of the composite columns: concrete-encased steel section columns and concrete-filled steel tube (CFT) columns [1]. The advantages of composite columns are high strength, stiffness, ductility, fire resistance and seismic resistance [2, 3]. Steel tubes with different cross-sections (rectangular, square, polygon and circular) are used to construct CFT columns [4, 5]. Circular steel tube sections are usually preferred for the CFT columns because circular steel tubes provide better confinement to the infill concrete [6]. In traditional CFT columns, steel tubes are usually filled with concrete without any internal steel reinforcement [7]. In some cases, internal steel reinforcement is used for higher strengths and better connections between the concrete members [8].

Reinforced concrete (RC) columns are usually constructed of normal-vibrated concrete (NVC). However, the congestion of reinforcement in the construction of columns is a critical issue. Casting concrete in columns with a large amount of longitudinal and transverse reinforcements makes the placement of concrete difficult. For such columns, the self-compacting concrete (SCC) is considered a suitable option to overcome the difficulty of the placement of concrete because SCC possesses good workability with high flowability, passing

ability and segregation resistances [9]. The SCC can be easily poured into narrow, complex or novel forms of construction without requiring vibration even in columns containing a large amount of reinforcement [10, 11].

Lin et al. [12] examined the behaviour of axially loaded RC columns constructed of NVC and SCC. Test results showed that the ductility, stiffness and crack control ability of the SCC columns were better than NVC columns. Lachemi et al. [13] examined the performance of axially loaded CFT columns constructed of NVC and SCC. Two series of steel tube confined concrete columns with and without longitudinal and transverse reinforcement were tested. The test results showed that axial load carrying capacities of NVC columns and SCC columns were comparable. Also, the casting of columns with SCC was easier than casting of columns with NVC, as SCC did not require any vibration.

Recently, the authors proposed a new method of reinforcing SCC columns with small diameter steel tubes as longitudinal reinforcement [14]. The behaviour of SCC columns reinforced with steel tubes is different from the behaviour of SCC columns reinforced with conventional steel bars. For the same cross-sectional area, the radius of gyration of the steel tube is higher than the radius of gyration of the solid steel bar. Steel tubes filled with SCC decreased the overall buckling of longitudinal reinforcement and consequently increased the ductility of the SCC columns. Also, steel tubes effectively confined the infill concrete resulting in an increase of the axial compressive strength. Under concentric axial load, steel tubes with a tensile strength similar to that of steel bars used in reinforcing SCC columns increased the maximum axial load of the column [14]. However, no analytical investigations have yet been carried out for the influence of different parameters (e.g., the compressive

strength of SCC, tensile strength of steel tube, wall thickness of steel tube and pitch of steel helix) on the behaviour of SCC columns reinforced with steel tubes.

Detailed analytical investigations are required for the wide use of SCC columns reinforced with steel tubes. This paper develops an analytical model to predict the axial load-axial deformation behaviour of SCC columns reinforced with steel tubes. The results of the analytical model have been found well matching with the experimental investigation results. The influences of the compressive strength of SCC, tensile strength of steel tube, wall thickness of steel tube and pitch of steel helix on the axial load-axial deformation behaviour of SCC columns reinforced with steel tubes have been investigated.

## **2. Research significance**

This study presents a simplified analytical model for the axial load-axial deformation behaviour of SCC columns reinforced with steel tubes. The analytical model takes into account the contributions of the steel tubes, unconfined concrete cover, confined concrete core and confined concrete inside the steel tube. The predictions of the developed analytical model have been found to be in good agreement with the experimental investigation results. The analytical observations, based on a detailed parametric study, reported in this study will contribute to good understanding on the axial load-axial deformation behaviour of SCC columns reinforced with steel tubes.

## **3. Analytical modelling**

The authors have recently proposed using small diameter steel tubes as longitudinal reinforcement for SCC columns. The innovative use of steel tubes for reinforcing SCC column was found to be highly effective, especially considering the maximum axial load and

the ductility of the SCC columns [14]. The conventional SCC columns reinforced with steel bars usually consist of three main components: longitudinal steel bars, unconfined concrete cover and confined concrete core (Fig. 1a). The SCC columns reinforced with steel tubes consist of four main components: longitudinal steel tubes, unconfined concrete cover, confined concrete core and confined concrete inside the steel tubes (Fig. 1b).

### 3.1 Modelling of longitudinal steel tubes

A simplified stress-strain relationship is used in the analytical model of the longitudinal steel tubes. The stress-strain behaviour of the steel tubes under tension and compression is idealized as bilinear elasto-plastic (Equations 1a and 1b). The strain hardening response of the longitudinal steel tube was neglected for a simplified analytical model.

$$f_t = \varepsilon_t E_t \quad \varepsilon_t \leq \varepsilon_{ty} \quad (1a)$$

$$f_t = f_{ty} \quad \varepsilon_t > \varepsilon_{ty} \quad (1b)$$

where  $f_t$  is the stress of the steel tube,  $\varepsilon_t$  is the axial strain corresponding to the  $f_t$ ,  $f_{ty}$  is the yield stress of the steel tube,  $\varepsilon_{ty}$  is the axial strain corresponding to the  $f_{ty}$  and  $E_t$  is the modulus of elasticity of the steel tube.

### 3.2 Modelling of unconfined concrete cover

The stress-strain behaviour of self-compacting concrete (SCC) in Aslani and Nejadi [15] is adopted to model the stress-strain behaviour of unconfined concrete cover in the SCC column. The stress-strain behaviour (Equation 2) of the SCC in Aslani and Nejadi [15] is divided into two branches: ascending (Equation 3a) and descending (Equation 3b).

$$f_c = \frac{f_{co} n (\varepsilon_c / \varepsilon_{co})}{n - 1 + (\varepsilon_c / \varepsilon_{co})^n} \quad (2)$$

$$n = n_1 = [1.02 - 1.17(E_{sec,u}/E_c)]^{-0.74} \quad \text{if } \varepsilon_c \leq \varepsilon_{co} \quad (3a)$$



$$n = n_2 = n_1 + (\varpi + 28 \times \xi) \quad \text{if } \varepsilon_c > \varepsilon_{co} \quad (3b)$$

$$E_c = 3655 \times (f_{co})^{0.548} \quad (\text{MPa}) \quad (4)$$

$$\varpi = (135.16 - 0.1744 \times f_{co})^{-0.46} \quad (5)$$

$$\xi = 0.83 \exp(-911/f_{co}) \quad (6)$$

$$E_{sec,u} = \frac{f_{co}}{\varepsilon_{co}} \quad (7)$$

$$\varepsilon_{co} = \left( \frac{f_{co}}{E_c} \right) \left( \frac{\psi}{\psi-1} \right) \quad (8)$$

$$\psi = \left( \frac{f_{co}}{17} \right) + 0.8 \quad (9)$$

where  $\varepsilon_c$  is the axial strain at any unconfined concrete stress  $f_c$ ;  $f_{co}$  is the unconfined concrete compressive strength;  $\varepsilon_{co}$  is the axial strain corresponding to  $f_{co}$ ;  $E_c$  is the modulus of elasticity of SCC (with fly ash filler);  $E_{sec,u}$  is the secant modulus of elasticity of unconfined concrete;  $n$  is the material parameter depending on the shape of the stress-strain curve;  $n_1$  and  $n_2$  are the modified material parameters at the ascending and descending branches, respectively; and  $\varpi$ ,  $\xi$  and  $\psi$  are coefficients of equations expressed in term of  $f_{co}$ .

The unconfined concrete compressive strength  $f_{co}$  is considered equal to 28-day cylinder compressive strength ( $f'_c$ ), multiplied by a coefficient  $\alpha_1$  according to AS 3600 [16]. The coefficient  $\alpha_1$  is expressed as:

$$\alpha_1 = 1.0 - 0.003f'_c \quad (f'_c \text{ in MPa}) \quad 0.72 \leq \alpha_1 \leq 0.85 \quad (10)$$

### 3.3 Modelling of confined concrete

Two confined concrete models need to be used in the modelling SCC columns reinforced with longitudinal steel tubes for the stress-strain behaviour of confined concrete core and confined concrete inside the steel tubes. The concrete stress-strain model in Mander et al. [17] is adopted to model the stress-strain behaviour of confined concrete core (Equation 11).

$$f_{cc} = \frac{f'_{cc} r_c (\varepsilon_{cc}/\varepsilon'_{cc})}{r_c - 1 + (\varepsilon_{cc}/\varepsilon'_{cc})^{r_c}} \quad (11)$$

$$r_c = \frac{E_c}{E_c - E_{sec,c}} \quad (12)$$

$$E_{sec,c} = \frac{f'_{cc}}{\varepsilon'_{cc}} \quad (13)$$

where  $\varepsilon_{cc}$  is the axial strain in concrete at any confined concrete stress  $f_{cc}$ ,  $\varepsilon'_{cc}$  is the axial strain at the peak stress of confined concrete  $f'_{cc}$ , and  $E_{sec,c}$  is the secant modulus of elasticity of the confined concrete. The  $f'_{cc}$  and  $\varepsilon'_{cc}$  are calculated using Equations (14) and (15), respectively.

$$f'_{cc} = f_{co} \left( 2.254 \times \sqrt{1 + \frac{7.94 f_l}{f_{co}}} - \frac{2 f_l}{f_{co}} - 1.254 \right) \quad (14)$$

$$\varepsilon'_{cc} = \varepsilon_{co} \left[ 1 + 5 \left( \frac{f'_{cc}}{f_{co}} - 1 \right) \right] \quad (15)$$

The ultimate confined concrete compressive strength in Mander et al. [17] is usually used with normal strength concrete having a compressive strength ranging between 27 and 31 MPa. However, for concrete with the compressive strengths higher than 31 MPa, Bing et al. [18] adjusted the peak stress of confined concrete  $f'_{cc}$  with a modification factor  $\alpha_s$  (Equation 16), which has been adopted herein.

$$f'_{cc} = f_{co} \left( 2.254 \times \sqrt{1 + \frac{7.94 \alpha_s f_l}{f_{co}}} - \frac{2 \alpha_s f_l}{f_{co}} - 1.254 \right) \quad (16)$$

$$\alpha_s = (21.2 - 0.35 f_{co}) \frac{f_l}{f_{co}} \quad \text{when } f_{co} \leq 52 \text{ MPa} \quad (17)$$

$$\alpha_s = 3.1 \frac{f_l}{f_{co}} \quad \text{when } f_{co} > 52 \text{ MPa} \quad (18)$$

where  $f_l$  is the effective confining pressure of the steel helix, which is calculated as:

$$f_l = \frac{1}{2} k_e \rho_{sh} f_{yh} \quad (19)$$

$$\rho_{sh} = \frac{4 A_{sh}}{s D_c} \quad (20)$$

$$k_e = \frac{1 - \frac{s'}{2D_c}}{1 - \rho_{cc}} \quad (21)$$

where  $f_{yh}$  is the yield stress of steel helix,  $\rho_{sh}$  is the volumetric ratio of steel helix,  $A_{sh}$  is the area of steel helix,  $D_c$  is the centre-to-centre diameter of steel helix,  $k_e$  is the coefficient of the fully confined concrete core by steel helix,  $\rho_{cc}$  is the ratio of longitudinal steel area to the concrete core area,  $s$  is the centre-to-centre spacing (pitch) of steel helix and  $s'$  is the clear spacing between the turns of steel helix.

The concrete stress-strain behaviour in Mander et al. [17] is also adopted to model the stress-strain behaviour of confined SCC inside the steel tube. However, the effective confining pressure provided by the steel tube is different from the effective confining pressure provided by the steel helix. The steel helix mainly provides confining pressure to the concrete core, whereas the steel tube resists axial stresses in addition to providing confinement to the concrete inside the steel tube. The common assumption adopted for the maximum confining pressure is that the steel helix will reach the yield stress [17]. This assumption may not be applicable for the confining pressure provided by the steel tube. Thus, the effective confining pressure provided by the steel tube is calculated based on the equilibrium of forces using Equation (22).

$$f_{lt} = \frac{2\sigma_{\theta}t}{d_t - 2t} \quad (22)$$

where  $\sigma_{\theta}$  is the hoop stress of the steel tube,  $d_t$  is the outside diameter of the steel tube, and  $t$  is the wall thickness of the steel tube. It is noted that a similar equation is also used for CFT columns [19]. However, the hoop stress of the steel tube in SCC columns reinforced with steel tubes is different from the hoop stress of the CFT columns because steel tubes in SCC columns reinforced with steel tubes are subjected to the restraining effect provided by the

concrete around the steel tube. The hoop stress of the steel tube in the SCC column reinforced with steel tubes is calculated as:

$$\sigma_{\theta} = \varepsilon_{\theta} E_t \quad (23)$$

where  $\varepsilon_{\theta}$  is the hoop strain of the steel tube and  $E_t$  is the modulus of elasticity of the steel tube.

A hoop strain factor ( $\alpha_{\theta}$ ) has been defined herein as:

$$\alpha_{\theta} = \sigma_{\theta} / f_{ty} \quad (24)$$

The  $\alpha_{\theta}$  of the CFT columns ranged 0.10 to 0.19 [20, 21]. However, the  $\alpha_{\theta}$  of steel tube in SCC columns reinforced with steel tubes is higher than the  $\alpha_{\theta}$  of the CFT columns. This is because additional confining pressures are provided to the steel tube by the steel helix and the concrete around the steel tube in SCC columns reinforced with steel tubes.

#### 3.4 Analytical axial load-axial deformation behaviour

The axial load-axial deformation response of SCC columns reinforced with steel tubes is calculated based on the developed stress-strain responses of the SCC and steel tubes. For an axial strain, the stress in each component (longitudinal steel tubes, unconfined concrete cover, confined concrete core and confined concrete inside the steel tubes) is calculated (Fig. 2a). The axial deformation of the specimen is calculated by multiplying the considered axial strains with the total length of the specimen. The axial load contribution of each component is calculated by multiplying the stresses of each component with the respective cross-sectional area (Fig. 2b). The steel helices essentially influence the stress-strain behaviour of the confined concrete core. The steel helices also influence the hoop strain of the longitudinal steel tubes. The influence of the pitch of steel helices is accounted for in the confined SCC inside the steel tubes. The effective confining pressure ( $f_{it}$ ) provided by the steel tube is calculated based on the experimentally determined hoop strain (average strains of strain

gauges at the maximum axial load) of the steel tube ( $\varepsilon_{\theta}$ ). The total axial load of the SCC columns reinforced with steel tubes is calculated as:

$$P_{axial} = f_t A_t + f_{c,cover} A_{cover} + f_{cc,core} A_{core} + f_{cc,tube} A_{tube} \quad (25)$$

where  $P_{axial}$  is the total axial load of specimens;  $f_t$ ,  $f_{c,cover}$ ,  $f_{cc,core}$  and  $f_{cc,tube}$  are the axial stresses in the longitudinal steel tubes, unconfined concrete cover, confined concrete core and confined concrete inside steel tubes, respectively;  $A_t$ ,  $A_{cover}$ ,  $A_{core}$  and  $A_{tube}$  are the cross-sectional areas of longitudinal steel tubes, unconfined concrete cover, confined concrete core and confined concrete inside steel tubes, respectively.

#### 4. Experimental axial load-axial deformation behaviour

A total of four SCC column specimens reinforced with steel tubes were cast and tested under monotonic axial compression. All specimens were tested at the Structural Engineering Laboratories, School of Civil, Mining and Environmental Engineering, University of Wollongong, Australia. The details of the experimental program including the design of experiments, preparation and testing, failure modes and behaviour of the specimens under concentric, eccentric and flexural loads were presented in Hadi et al. [14].

##### 4.1 Details of the column specimens

All specimens were 240 mm in diameter and 800 mm in height. The SCC mix with a nominal compressive strength of 50 MPa and a maximum aggregate size of 10 mm were used in casting the specimens. The first and second specimens were reinforced longitudinally with ST33.7 steel tubes. The ST33.7 steel tube had 33.7 mm outside diameter, 2 mm wall thickness and 350 MPa nominal tensile strength. The first and second specimens were reinforced transversely with 50 mm and 75 mm pitch of the steel helices, respectively. The third and fourth specimens were reinforced longitudinally with ST26.9 steel tubes. The ST26.9 steel

tube had 26.9 mm outside diameter, 2.6 mm wall thickness and 250 MPa nominal tensile strength. The third and fourth specimens were also reinforced transversely with 50 mm and 75 mm pitch of the steel helices, respectively. Both ST33.7 and ST26.9 steel tubes had approximately the same cross-sectional area. All specimens were reinforced transversely with R10 bar (10 mm diameter plain steel bar) with a nominal tensile strength of 250 MPa.

The SCC column specimens were labelled according to the type of longitudinal steel tubes and the pitch of the steel helix (Table 1). In the specimen label, ST33.7 and ST26.9 refer to the type of the steel tubes. Afterwards, H50 and H75 represent 50 mm and 75 mm pitch of the steel helices, respectively. The letter C at the end of the specimen label represents that the specimen was tested under concentric axial load. For example, ST26.9H50C refers to the column specimen reinforced longitudinally with ST26.9 steel tubes and transversely with 50 mm pitch of the steel helix and tested under concentric axial load. Table 1 provides details of the column specimens included in this study.

#### 4.2 Materials properties

The properties of fresh self-compacting concrete (SCC) were tested according to ASTM C1621/C1621M [22], ASTM C1611/C1611M [23] and ASTM C1610/C1610M [24]. The compressive strength of the SCC was determined by testing three cylinders of 100 mm diameter and 200 mm height according to ASTM C39/C39M [25]. The average 28-day compressive strength of the SCC was 57 MPa. Two different steel tubes were used for steel tube reinforced SCC specimens: ST33.7 and ST26.9. Three samples from each of ST33.7 and ST26.9 tubes were tested according to ASTM A370 [26]. Yield stresses of both steel tubes were determined using the 0.2% offset method, as clearly defined yield stress was not observed. The average yield stress ( $f_{ty}$ ), yield strain ( $\epsilon_{ty}$ ) and modulus of elasticity ( $E_t$ ) of

ST33.7 steel tube were found as 450 MPa, 0.23% and 196 GPa, respectively. The average yield stress, yield strain and modulus of elasticity of ST26.9 steel tube were found as 355 MPa, 0.187% and 192 GPa, respectively.

Rounded steel R10 helices were used as transverse reinforcement in all of the specimens. Three samples of R10 rounded steel bars (gauge length 340 mm) were tested according to Australian Standard AS 1391 [27]. The yield stress of rounded steel bar was determined using the 0.2% offset method, as clearly defined yield stress was not observed. The average yield stress ( $f_{yh}$ ), yield strain ( $\varepsilon_{yh}$ ) and modulus of elasticity ( $E_{yh}$ ) of R10 bars were found as 400 MPa, 0.22% and 195 GPa, respectively.

#### 4.3 Instrumentation

The test specimens were instrumented internally and externally to measure the strains of reinforcements (steel tubes and steel helices) and axial deformations of specimens. In order to observe the axial strains of longitudinal steel tubes, strain gauges were attached on the two opposite longitudinal steel tubes. Also, to observe the lateral strains of transverse reinforcement, two strain gauges were attached to the two opposite sides of the steel helices. All strain gauges were attached to the external faces of the longitudinal and transverse reinforcements at the midheight of the specimens. Two types of strain gauges were used in this study: single element strain gauges were used for steel helices and biaxial two element strain gauges were used for steel tubes. Biaxial two element strain gauges were used to measure both the axial and the lateral strains of the longitudinal steel tube. The biaxial two element strain gauges were placed at the mid-height of the steel tubes ensuring that they were centrally placed between two turns of the helix. Figure 3 shows the schematic of the positions of single element strain gauges and biaxial two element strain gauges on the test specimens.

The test specimens were instrumented with two linear variable differential transducers (LVDTs) fixed diagonally at opposite corners in the testing machine to measure the axial deformations. All specimens were tested in a 5000 kN compression testing machine. Testing was carried out at a displacement controlled loading rate of 0.3 mm/min until the failure of the specimen.

### 5. Experimental results of the SCC column specimens

Experimental results of four SCC column specimens tested under concentric axial load in terms of yield axial load and corresponding axial deformation, maximum axial load and corresponding axial deformation and ultimate axial deformation are presented in Table 1. The ultimate axial deformation corresponds to the deformation at the fracture of steel helices. Although the cross-sectional areas of the ST33.7 and ST26.9 steel tubes are similar, the yield axial load of Specimen ST33.7H50C was 5% greater than the yield axial load of Specimen ST26.9H50C and the maximum axial load of Specimen ST33.7H50C was 4.8% greater than the maximum axial load of Specimen ST26.9H50C. The greater yield and maximum axial load of specimen reinforced with ST33.7 steel tubes were because the ST33.7 steel tube had higher tensile strength than the ST26.9 steel tube. Besides, the ST33.7 steel tube had large inside and outside diameters compared to the ST26.9 steel tube. The large inside diameter of the ST33.7 steel tube allowed a large amount of concrete to be filled inside the tube which contributed in increasing the compressive strength of the column specimens. The large outside diameter of ST33.7 steel tube had a lower slenderness ( $s/d_t$ ) ratio which positively contributed to the maximum axial load of Specimen ST33.7H50C.

Table 2 reports the strains in the longitudinal and transverse reinforcements for all tested specimens. In Column 1 of Table 2, the letters SA, SL and SH refer to the strain gauges that



were placed on the steel tubes in the longitudinal direction, on the steel tubes in the lateral direction and on the steel helix in the lateral direction, respectively. The numbers 1 and 2 afterwards refer to the first and second strain gauges, respectively. The averages of the recorded strains are also reported in Table 2. The average axial strains in the longitudinal steel tubes indicated that the steel tubes yielded at the maximum axial load. Also, it was found that the contribution of ST33.7 steel tubes was 29.8% of the maximum axial load of Specimen ST33.7H50C, whereas the contribution of ST33.7 steel tubes was 27.6% of the maximum axial load of Specimen ST33.7H75C. The contribution of ST26.9 steel tubes was 30.7% of the maximum axial load of Specimen ST26.9H50C, whereas the contribution of ST26.9 steel tubes was 24.5% of the maximum axial load of Specimen ST26.9H75C. The maximum axial load of steel tubes filled with concrete decreased with the increase in the  $s/d_t$  ratio of steel tubes [11, 28]. Thus, increasing  $s/d_t$  ratio of the steel tubes resulted in the lower contributions of steel tubes in the maximum axial load of the tested column specimen.

The compressive strength of the confined concrete core and the compressive strength of the confined concrete inside the steel tube have been compared. It has been observed that steel tubes effectively confined the concrete inside the tube and resulted in higher axial compressive strengths of the SCC columns. To compare the compressive strength of the confined concrete core ( $f_{cc,core}$ ) and confined concrete inside the steel tube ( $f_{cc,tube}$ ), the enhancement factor of the confined concrete core ( $f_{cc,core}/f_{co}$ ) and the confined concrete inside the steel tube ( $f_{cc,tube}/f_{co}$ ) were calculated based on the developed stress-strain behaviours of the SCC and steel tubes (Table 3). The unconfined concrete strength ( $f_{co}$ ) is taken as 0.95 times the 28-day cylinder compressive strength for concrete inside the steel tubes [29]. For the concrete core confined by steel helix, the enhancement factors were 1.32 and 1.13 for the pitch of steel helices of 50 and 75 mm, respectively. However, for the

confined concrete inside ST33.7 steel tube, the enhancement factors were 2.6 and 2.25 for the pitch of steel helices of 50 and 75 mm, respectively. Also, for confined concrete inside the ST26.9 steel tube, the enhancement factors were 3.41 and 2.34 for the pitch of steel helices of 50 and 75 mm, respectively. It can be observed that the enhancement factors of the confined concrete inside steel tubes were higher than the enhancement factors of the confined concrete core for the same pitch of steel helices. The enhancement factor is higher inside the steel tube, which is because the concrete inside the steel tube was effectively confined by the wall of steel tube as well as the steel helix and the concrete around the steel tube.

The enhancement factor of confined concrete inside the ST26.9 steel tube was 31% more than the enhancement factor of confined concrete inside the ST33.7 steel tube, when the pitch of steel helix was 50 mm. The enhancement factor of the concrete inside the steel tube was larger for smaller diameter steel tube, as the strength of confined concrete inside the steel tube increased with decreasing the diameter of the steel tube [4]. Also, outside diameter to thickness ( $d_t/t$ ) ratio of the ST26.9 steel tube was 10.35, whereas the  $d_t/t$  ratio of the ST33.7 steel tube was 16.85. The lower  $d_t/t$  ratio of steel tube provided higher confinement to the concrete inside the steel tube [30]. The steel helix also provided confinement to the steel tubes in the SCC column. This additional confinement by steel helix resulted in restricting the lateral dilation of the steel tube due to axial compression at the connecting area between the steel helix and steel tubes. Thus, the confinement of concrete inside steel tubes also decreases with the increase of the steel helix pitch.

## 6. Analytical versus experimental results

The analytical and experimental axial load-axial deformation behaviours of the SCC column specimens reinforced with steel tubes are compared (Fig. 4). For all the column specimens,

for the ascending part of the curve up to the maximum axial load, the analytical axial load-axial deformation curve correlated well with the experimental axial load-axial deformation curve. This good correlation is particularly because the stress-strain response of the different components of the specimens up to the maximum axial load was relatively linear. It can also be observed that, after the maximum axial load, the descending parts of the analytical axial load-axial deformation curves show good agreements with the experimental axial load-axial deformation curves. The experimental axial load-axial deformation curve shows a small drop and a rise in the descending part of the curve. However, the analytical axial load-axial deformation curve shows a gradual decrease in the descending part of the curve. The small drop in the experimental axial load-axial deformation curve has not been captured by the analytical curve, as the drop occurred instantaneously due to the spalling of concrete cover and then the axial load increased to a value less than the maximum axial load due to the confinement provided by the steel helices.

## 7. Parametric study

The developed analytical model was used to study the influences of different parameters on the axial load-axial deformation behaviours of SCC columns reinforced with steel tubes. The parameters studied were the compressive strength of SCC, tensile strength of steel tube, wall thickness of steel tube and pitch of steel helix.

### 7.1 Effect of concrete compressive strength

Four different concrete compressive strengths (30, 40, 50 and 60 MPa) were considered. The SCC columns were reinforced longitudinally with either ST33.7 steel tube or ST26.9 steel tube and transversely with 50 mm pitch of steel helix. The tensile strengths of ST33.7 and

ST26.9 steel tubes were 450 MPa and 355 MPa, respectively, which were similar to the yield strength of the steel tubes used in reinforcing the tested column specimens.

The influence of concrete strength on the axial load-axial deformation behaviours of the SCC columns is shown in Fig. 5. As expected, the maximum axial load of the SCC columns reinforced with steel tubes increased with the increase in the compressive strength of concrete. It was observed that as the concrete compressive strength increased from 30 MPa to 60 MPa, the maximum axial load of the columns reinforced with ST33.7 and ST26.9 steel tubes increased by about 27.7% and 30.5%, respectively (Table 4). This is particularly because increasing the strength of concrete increased the contribution of the concrete to the maximum axial load of the column. Also, the maximum axial load of the steel tubes filled with concrete increased with increasing concrete strength [7]. For the descending part of the axial load-axial deformation response, the slope of the axial load-axial deformation curve after the maximum axial load increased with the increase in the concrete strength. Ozbakkaloglu and Saatcioglu [31] reported that the reduction in the axial load capacity after the peak load was a function of the concrete strength and the rate of drop in the axial load carrying capacity increased with increasing concrete strength.

The ductility of columns was significantly influenced by the increase in the compressive strength of concrete. The ductility is an indication of the ability of the structural members to undergo large deformations before failure. In this study, the ductility was calculated as a ratio of the axial deformation at the first helix fracture ( $\delta_u$ ) to the axial yield deformation ( $\delta_y$ ) [32], as in Equation (26). The  $\delta_y$  represents the deformation corresponding to the intersection point of a horizontal line from the maximum axial load and an extension secant line from the original point and the point at 0.75 times the maximum axial load [33].

$$Ductility = \delta_u / \delta_y \quad (26)$$

In this study, the analytical axial load-axial deformation curves matched well with the experimental axial load-axial deformation curves. Consequently, the ductility of the specimens obtained from the analytical investigations was very similar to the ductility of the specimens obtained from the experimental investigations. It was observed that as the compressive strength of concrete increased from 30 MPa to 60 MPa, the ductility of Specimen ST33.7H50C decreased by about 19.4%, whereas the ductility of Specimen ST26.9H50C decreased by about 22.2% (Table 4). For the increase in the compressive strength of concrete from 30 MPa to 60 MPa, columns reinforced with ST26.9 steel tubes showed a rapid descending axial load-axial deformation curve than columns reinforced with ST33.7 steel tubes. The  $s/d_t$  ratio of Specimen ST26.9H50C was 20% higher than the  $s/d_t$  ratio of Specimen ST33.7H50C, as the outside diameter of the ST26.9 steel tube was smaller than the outside diameter of the ST33.7 steel tube. Increasing  $s/d_t$  ratio of columns caused an increase in the slope of the post peak axial load-axial deformation of the column (Fig. 5).

### 7.2 Effect of tensile strength and wall thickness of the steel tube

Steel tubes with four different tensile strengths (300, 400, 500 and 600 MPa) and with four different wall thicknesses (1.5, 2.0, 2.5 and 3.0 mm) were considered. The SCC columns were reinforced longitudinally with either ST33.7 steel tube or ST26.9 steel tube and transversely with 50 mm pitch of steel helix. The compressive strength of the SCC was considered 57 MPa which was similar to the compressive strength of the SCC used in casting the tested column specimens. The influence of tensile strength of steel tubes on axial load-axial deformation behaviours for the SCC columns is shown in Fig. 6. It was observed that the tensile strength of the steel tubes did not influence the overall trend of the axial load-axial deformation behaviour of the SCC columns. However, it was observed that as the tensile strength of

longitudinal steel tubes increased from 300 MPa to 600 MPa, the maximum axial load of Specimens ST33.7H50C and ST26.9H50C increased by about 15.7% and 14.7%, respectively (Table 5). The higher strength of longitudinal steel tubes increased the contribution of steel tube in carrying the axial load of the column.

The influence of wall thicknesses of steel tubes on axial load-axial deformation behaviours for the SCC columns is shown in Fig. 7. The thicknesses of steel tubes did not significantly influence the overall trend of the axial load-axial deformation behaviour of the columns. However, the maximum axial load of the SCC columns was increased with the increase in the wall thickness of steel tubes. It was observed that as the wall thickness of steel tubes increased from 1.5 mm to 3.0 mm, the maximum axial load of the columns reinforced with ST33.7 steel tubes increased by about 13.8% whereas the maximum axial load of the columns reinforced with ST26.9 steel tubes increased by about 8.4% (Table 6). The reason for the differences in the maximum axial load is associated with the cross-sectional area of the steel tube. The cross-sectional area of the ST33.7 steel tube was 28.4% larger than the cross-sectional area of the ST26.9 steel tube, when the wall thickness of both steel tubes was considered 3 mm. The higher wall thickness of steel tube increased the cross-sectional area of the steel tube and increased the contribution of steel tube in carrying the axial load of the column. Also, increasing the wall thickness of steel tube increased the compressive strength of the concrete inside the steel tube and increased the compressive strength of the SCC column. The confinement of concrete inside the steel tube increased with decreasing  $d_t/t$  ratio of the steel tube.

The increase in the tensile strength and wall thickness of steel tube increased the maximum axial load of the columns. However, the ductility of the SCC columns was not increased

significantly. For the increase of the wall thickness of steel tubes in the SCC columns from 1.5 mm to 3.0 mm, the ductility of the SCC columns reinforced with steel tubes increased by only 6% (Table 6). Although increasing the wall thickness of steel tube resulted in an increase in the strength and ductility of concrete inside the steel tubes, the concrete inside the steel tubes was a small proportion of the total cross-sectional area of the column.

### 7.3 Effect of pitch of steel helices

Four different pitches of steel helices (40, 60, 80 and 100 mm) were considered. The SCC columns were reinforced longitudinally with either ST33.7 steel tube or ST26.9 steel tube. The tensile strengths of ST33.7 and ST26.9 steel tubes were 450 MPa and 355 MPa, respectively. The compressive strength of the SCC was 57 MPa.

The influence of different pitch of steel helices on axial load-axial deformation behaviours of the SCC columns is shown in Fig. 8. All columns showed the same initial behaviour up to the maximum axial load. However, for the increase of the pitch of steel helices from 40 to 100 mm in the SCC columns reinforced with ST26.9 steel tubes, the maximum axial load decreased by 10.3% (Table 4). Whereas increasing the pitch of steel helices from 40 to 100 mm in the SCC columns reinforced with ST33.7 steel tubes, the maximum axial load decreased by 6.9% (Table 7). The reason for the differences in the maximum axial loads is associated with the  $s/d_t$  ratio of steel tubes. The  $s/d_t$  ratio of the ST26.9 steel tube was 25% higher than the  $s/d_t$  ratio of the ST33.7 steel tube when the pitch of steel helix was 100 mm.

It was observed that for increasing the pitch of steel helices from 40 to 100 mm in the SCC columns reinforced with ST26.9 steel tubes, the ductility decreased by 40% (Table 7). Whereas increasing the pitch of steel helices from 40 to 100 mm in the SCC columns

reinforced with ST33.7 steel tubes, the ductility decreased by 37% (Table 7). The higher ductility of the column transversely reinforced with a smaller pitch steel helices is mainly attributed to the delay in the first helix fracture compared to the early first helix fracture of the column transversely reinforced with a larger pitch steel helices. Increasing the pitch of steel helices from 40 to 100 mm in the SCC columns resulted in the increase of the  $s/d_t$  ratio of steel tubes. The ability of the column transversely reinforced with closely spaced steel helix in sustaining the lateral pressure provided by the longitudinal steel tubes under axial compression was higher than the ability of the column transversely reinforced with largely spaced steel helix. The lateral pressure exerted by the longitudinal steel tubes in the largely spaced steel helix resulted in the early yielding and fracturing of steel helix. Also, increasing the pitch of steel helices from 40 to 100 mm significantly influenced the descending part of the axial load-axial deformation behaviour of the SCC column and resulted in an increase of the slope of the post-peak axial load-axial deformation curve (Fig. 8). It is noted that experimental investigations are required for very small and very large pitches of steel helices to verify the results of analytical modeling. Such experimental investigations are part of the ongoing research project by the authors.

## 7. Conclusions

This study presents analytical investigations on the axial load-axial deformation behaviour of self-compacting concrete (SCC) columns reinforced with steel tubes. Two types of steel tubes were used in the SCC columns as longitudinal reinforcement. The influences of different parameters including the compressive strength of SCC, tensile strength of steel tube, wall thickness of steel tube and pitch of steel helix were investigated. Based on the analytical results of this study, the following conclusions are drawn:



1. The analytical axial load-axial deformation response of the SCC columns reinforced with steel tubes was calculated based on the stress-strain responses of the longitudinal steel tubes, unconfined concrete cover, confined concrete core and confined concrete inside the steel tube. The analytical and experimental axial load-axial deformation curves of columns showed good agreements.

2. The compressive strength of the confined concrete core and the compressive strength of the confined concrete inside the steel tube were compared. For the SCC columns reinforced transversely with steel helices having a pitch of 50 mm, the enhancement factor of the confined concrete core was 1.32, whereas the enhancement factors of the confined concrete inside the ST33.7 and ST26.9 steel tubes were 2.6 and 3.41, respectively. The enhancement factors of the confined concrete inside the steel tubes were higher than the enhancement factors of the confined concrete core for the same pitch of steel helices. Thus, steel tubes effectively confined the concrete inside the tube and resulted in higher axial compressive strengths of the SCC columns.

3. As the concrete compressive strength increased from 30 MPa to 60 MPa, the maximum axial load of the SCC columns reinforced with ST33.7 and ST26.9 steel tubes increased by about 27.7% and 30.5%, respectively. With the increase in the compressive strength of concrete from 30 MPa to 57 MPa, the ductility of Specimen ST33.7H50C decreased by about 19.4%, whereas the ductility of Specimen ST26.9H50C decreased by about 22.2%.

4. As the tensile strength of longitudinal steel tubes increased from 300 MPa to 600 MPa, the maximum axial load of Specimens ST33.7H50C and ST26.9H50C increased by about 15.7% and 14.7%, respectively. Also, as the wall thickness of longitudinal steel tubes increased from 1.5 mm to 3.0 mm, the maximum axial load of the SCC columns reinforced with ST33.7 steel tubes increased by about 13.8%, whereas the maximum axial load of the SCC columns

reinforced with ST26.9 steel tubes increased by about 8.4%. However, the ductility of SCC columns reinforced with steel tubes was not significantly influenced by the increase in the tensile strength and wall thickness of steel tube.

5. For the increase of the pitch of steel helices from 40 to 100 mm in the SCC columns reinforced with ST26.9 steel tubes, the maximum axial load decreased by 10.3%. Whereas increasing the pitch of steel helices from 40 to 100 mm in the SCC columns reinforced with ST33.7 steel tubes, the maximum axial load decreased by 6.9%. The  $s/d_t$  ratio of the ST26.9 steel tube was 25% higher than the  $s/d_t$  ratio of the ST33.7 steel tube when the pitch of steel helix was 100 mm.

6. For the increase of the pitch of steel helices from 40 to 100 mm in the SCC columns reinforced with ST26.9 steel tubes, the ductility decreased by 40%. Whereas increasing the pitch of steel helices from 40 to 100 mm in the SCC columns reinforced with ST33.7 steel tubes, the ductility decreased by 37%.

### Acknowledgments

The authors thank the University of Wollongong, Australia and technical officers at the High Bay Laboratory, especially Mr. Ritchie McLean, for their help in the experimental work of this study. Finally, the first author would like to acknowledge the Iraqi Government for the support of his PhD scholarship.

**Notation**

$A_{core}$	= area of the concrete core confined by steel helix
$A_{cover}$	= area of unconfined concrete cover
$A_{sh}$	= cross-sectional area of the steel helix
$A_t$	= cross-sectional area of the steel tube
$A_{tube}$	= area of the confined concrete inside steel tubes
$D_c$	= centre-to-centre diameter of the steel helix
$d_t$	= outside diameter of the steel tube
$E_c$	= modulus of elasticity of the concrete
$E_{sh}$	= modulus of elasticity of the steel helix
$E_{sec,c}$	= confined secant modulus of elasticity of the concrete
$E_{sec,u}$	= unconfined secant modulus of elasticity of the concrete
$E_t$	= modulus of elasticity of the steel tube
$P_{axial}$	= total axial load of specimens
$f_c$	= unconfined concrete stress
$f'_c$	= 28-day cylinder concrete compressive strength
$f_{cc,core}$	= axial stress in the confined concrete core
$f_{cc,tube}$	= axial stress in the longitudinal steel tubes
$f_{cc}$	= confined concrete stress
$f'_{cc}$	= peak stress of confined concrete
$f_{co}$	= unconfined concrete compressive strength which is equal to $\alpha_1$ multiplied by $f'_c$
$f_l$	= effective confining pressure of steel helix
$f_{lt}$	= effective confining pressure of the steel tube
$f_t$	= stress of the steel tube in the linear elastic portion
$f_{ty}$	= yield stress of the steel tube
$f_{yh}$	= yield stress of the steel helix

- $k_e$  = coefficient of the fully confined concrete core by steel helix  
 $n_1$  = modified material parameter at the ascending part  
 $n_2$  = modified material parameters at the descending part  
 $s'$  = clear spacing of the steel helix  
 $n$  = material parameter depending on the shape of stress-strain curve  
 $s$  = pitch (centre-to-centre spacing) of the steel helix  
 $t$  = wall thickness of the steel tube  
 $\alpha_1$  = coefficient of concrete compressive strength, as given in AS 3600 [16]  
 $\alpha_s$  = modification factor for the peak stress of confined concrete  
 $\alpha_\theta$  = hoop strain factor  
 $\delta_u$  = axial deformation of the column at the first helix fracture  
 $\delta_y$  = axial yield deformation of the column  
 $\varepsilon_c$  = axial strain corresponding to  $f_c$   
 $\varepsilon_{cc}$  = axial strain corresponding to  $f_{cc}$   
 $\varepsilon'_{cc}$  = axial strain corresponding to  $f'_{cc}$   
 $\varepsilon_{co}$  = axial strain corresponding to  $f_{co}$   
 $\varepsilon_t$  = axial strain corresponding to  $f_t$   
 $\varepsilon_{ty}$  = axial strain corresponding to  $f_{ty}$   
 $\varepsilon_{yh}$  = axial strain corresponding to  $f_{yh}$   
 $\varepsilon_\theta$  = hoop strain of the steel tube  
 $\rho_{cc}$  = ratio of longitudinal steel area to core area  
 $\rho_s$  = longitudinal reinforcement ratio  
 $\rho_{sh}$  = volumetric ratio of steel helix  
 $\sigma_\theta$  = hoop stress of the steel tube  
 $\omega, \xi, \psi$  = coefficients of equations for model Aslani and Nejadi [15]

**Reference**

- [1] Wang YC. Tests on slender composite columns. *J Constr Steel Res* 1999; 49(1):25-41.
- [2] Susantha KAS, Ge H, Usami T. Uniaxial stress–strain relationship of concrete confined by various shaped steel tubes. *Eng Struct* 2001; 23(10):1331-1347.
- [3] Hajjar JF. Composite steel and concrete structural systems for seismic engineering. *J Constr Steel Res* 2002; 58(5-8):703-723.
- [4] Sakino K, Nakahara H, Morino S, Nishiyama I. Behavior of centrally loaded concrete-filled steel-tube short columns. *J Struct Eng ASCE* 2004; 130(2):180-188.
- [5] Han L-H, Li W, Bjorhovde R. Developments and advanced applications of concrete-filled steel tubular (CFST) structures: members. *J Constr Steel Res* 2014; 100:211-228.
- [6] Alhussainy F, Sheikh MN, Hadi MNS. Behavior of small diameter steel tubes under axial compression. *Structures J.* 2017; 11:155-163.
- [7] Oliveira, WLA, De Nardin S, El Debs ANC, El Debs MK. Influence of concrete strength and length/diameter on the axial capacity of CFT columns. *J Constr Steel Res* 2009; 65(12):2103-2110.
- [8] Moon J, Lehman D, Roeder C, Lee H. Strength of circular concrete-filled tubes with and without internal reinforcement under combined loading. *J Struct Eng ASCE* 2013; 139(12):1-12.
- [9] EFNARC. Specification and guidelines for self-compacting concrete. The European Federation of Specialist Construction Chemicals and Concrete Systems 2002.
- [10] Paultre P, Khayat KH, Cusson D, Tremblay S. Structural performance of self-consolidating concrete used in confined concrete columns. *ACI Struct J* 2005; 102(4):560-568.

- [11] Alhussainy F, Hadi MNS, Sheikh MN. Behaviour of small-diameter self-compacting concrete-filled steel tubes. *Mag Concr Res* 2017; 1-11.  
<http://dx.doi.org/10.1680/jmacr.16.00531>
- [12] Lin C-H, Hwang, C-L, Lin S-P, Liu C-H. Self-consolidating concrete columns under concentric compression. *ACI Struct J* 2008; 105(4): 425-432.
- [13] Lachemi M, Hossain KMA, Lambros VB. Axial load behavior of self-consolidating concrete-filled steel tube columns in construction and service stages. *ACI Struct J* 2006; 103(1):38-47.
- [14] Hadi MNS, Alhussainy F, Sheikh MN. Behavior of self-compacting concrete columns reinforced longitudinally with steel tubes. *J Struct Eng ASCE* 2017; 143(6):1-14.
- [15] Aslani F, Nejadi S. Mechanical properties of conventional and self-compacting concrete: an analytical study. *Const Build Mater* 2012; 26:330-347.
- [16] AS 3600-09. Concrete structure. Australian Standard (AS), Sydney, 2009.
- [17] Mander JB, Priestley MJN, Park R. Theoretical stress-strain model for confined concrete. *J Struct Eng ASCE*; 1988; 114(8):1804-1826.
- [18] Bing L, Park R, Tanaka H. Stress-strain behavior of high-strength concrete confined by ultra-high- and normal-strength transverse reinforcements. *ACI Struct J* 2001; 98(3):395-406.
- [19] Wang X, Liu J, Zhang S. Behavior of short circular tubed-reinforced-concrete columns subjected to eccentric compression. *Eng Struct* 2015; 105:77-86.
- [20] Elremaily A, Azizinamini A. Behavior and strength of circular concrete-filled tube columns. *J Constr Steel Res* 2002; 58(12):1567-1591.
- [21] Morino S, Tasuda K. Design and construction of concrete-filled steel tube column system in Japan. *Earthq Eng and Eng Seismol* 2002; 4(1):51-73.

- [22] ASTM C1621/C1621M-14. Standard test method for passing ability of self-consolidating Concrete by J-Ring. West Conshohocken, PA, USA: American Society for Testing and Materials; 2014.
- [23] ASTM C1611/C1611M-14. Standard test method for slump flow of self-consolidating concrete. West Conshohocken, PA, USA: American Society for Testing and Materials; 2014.
- [24] ASTM C1610/C1610M-14. Standard test method for static segregation of self-consolidating concrete using column technique. West Conshohocken, PA, USA: American Society for Testing and Materials; 2014.
- [25] ASTM C39/C39M-16. Standard test method for compressive strength of cylindrical concrete specimens. West Conshohocken, PA, USA: American Society for Testing and Materials; 2016.
- [26] ASTM A370-14. Standard test method and definition for mechanical testing of steel products. West Conshohocken, PA, USA: American Society for Testing and Materials; 2014.
- [27] AS 1391-07. Metallic materials tensile testing at ambient temperature. Australian Standard (AS), Sydney; 2007.
- [28] Oliveira WLA, De Nardin S, El Debs ALHC, El Debs MK. Evaluation of passive confinement in CFT columns. *J Constr Steel Res* 2010; 66(4):487-495.
- [29] ANSI/AISC 360-10. Specification for structural steel buildings. American Institute of Steel Construction (AISC), Chicago; 2010.
- [30] Abed F, Alfaraydeh M, Abdalla S. Experimental and numerical investigations of the compressive behavior of concrete filled steel tubes (CFSTs). *J Constr Steel Res* 2013; 80:429-439.
- [31] Ozbakkaloglu T, Saatcioglu M. Rectangular stress block for high-strength concrete. *ACI Struct J* 2004; 101(4):475-483.

[32] Pessiki S, Pieroni A. Axial load behavior of large scale spirally reinforced high strength concrete columns. ACI Struct J 1997; 94(3):304-313.

[33] Foster SJ, Attard MM. Experimental tests on eccentrically loaded high-strength concrete columns. ACI Struct J 1997; 94(3):295-302.

**ACCEPTED MANUSCRIPT**



**List of tables:**

**Table 1**—Details and experimental results of four column specimens tested under concentric load

**Table 2**—The strains of the longitudinal and transverse reinforcements for the column specimens tested under concentric load

**Table 3**—The concrete enhancement factor for the types of confined concrete in the SCC columns

**Table 4**—Influence of the compressive strength of concrete on the maximum axial load and ductility of columns

**Table 5**—Influence of the tensile strength of steel tube on the maximum axial load and ductility of columns

**Table 6**—Influence of the wall thickness of steel tube on the maximum axial load and ductility of columns

**Table 7**—Influence of the pitch of steel helices on the maximum axial load and ductility of columns

ACCEPTED MANUSCRIPT

**List of figures:**

**Fig. 1**—Cross-sections of the self-compacting concrete columns: (a) column reinforced with steel bars; and (b) column reinforced with steel tubes

**Fig. 2**—Components in the columns reinforced with steel tubes: (a) axial stress-axial strain behaviour of each component; and (b) axial load-axial deformation behaviour of each component

**Fig. 3**—Positions of single element strain gauges and biaxial two element strain gauges on the test specimens

**Fig. 4**—Comparison between analytical and experimental axial load-axial deformation behaviour of the tested specimens: (a) ST33.7H50C; (b) ST26.9H50C; (c) ST33.7H75C; and (d) ST26.9H75C

**Fig. 5**—Influence of concrete strength on axial load-axial deformation behaviours of the SCC columns: (a) ST33.7H50C; and (b) ST26.9H50C

**Fig. 6**—Influence of tensile strength of steel tubes on axial load-axial deformation behaviours of the SCC columns: (a) ST33.7H50C; and (b) ST26.9H50C

**Fig. 7**—Influence of wall thicknesses of steel tubes on axial load-axial deformation behaviours of the SCC columns: (a) ST33.7H50C; and (b) ST26.9H50C

**Fig. 8**—Influence of pitch of steel helices on axial load-axial deformation behaviours of the SCC columns: (a) columns reinforced with ST33.7 steel tubes; and (b) columns reinforced with ST26.9 steel tubes

Table 1–Details and experimental results of four column specimens tested under concentric load

No.	Specimen Designation	Longitudinal Reinforcement			Transverse Reinforcement		Experimental Results				
		Outside Diameter of Steel Tubes mm	Thickness of Tubes mm	Reinf. Ratio $\rho_s$ (%)	Pitch mm	Reinf. Ratio $\rho_{sh}$ (%)	Yield axial load kN	Corresponding axial deformation mm	Maximum axial load kN	Corresponding axial deformation mm	Ultimate axial deformation* mm
1	ST33.7H50C	33.7	2	2.64	50	3.3	2500	2.45	2729	3.29	33.5
2	ST33.7H75C	33.7	2	2.64	75	2.2	2395	2.65	2633	3.44	26.2
3	ST26.9H50C	26.9	2.6	2.63	50	3.3	2375	2.35	2598	3.03	36
4	ST26.9H75C	26.9	2.6	2.63	75	2.2	2275	2.2	2443	2.79	30.4

\* Ultimate axial deformation was defined by the fracture of the steel helices.

**Table 2–The strains of the longitudinal and transverse reinforcements for the column specimens tested under concentric load**

Labels of strain gauges	Strain gauge reading corresponding to the maximum load (%)		
	ST33.7H50C	ST26.9H50C	ST33.7H75C ST26.9H75C
SA-1 (compression)	0.318	0.3	0.294 0.244
SA-2 (compression)	0.378	0.4	0.327 0.280
Average SA (compression)	0.348	0.35	0.311 0.262
SL-1 (tension)	0.092	0.059	0.070 0.045
SL-2 (tension)	0.088	0.093	0.078 0.043
Average SL (tension)	0.090	0.076	0.074 0.044
SH-1 (tension)	0.080	0.054	0.071 0.060
SH-2 (tension)	0.064	0.082	0.088 0.076
Average SH (tension)	0.072	0.068	0.080 0.068

Note:

SA refers to the strain gauges that were placed on the steel tubes in the longitudinal direction.

SL refers to the strain gauges that were placed on the steel tubes in the lateral direction.

SH refers to the strain gauges that were placed on the steel helix in the lateral direction.

Table 3–The concrete enhancement factor for the types of confined concrete in the SCC columns

Types of confined concrete in the specimens	Confined concrete [ $(f_{cc,core})$ or $(f_{cc,tube})$ ] MPa	Unconfined concrete ( $f_{co}$ ) MPa	concrete enhancement factor [ $(f_{cc,core}/f_{co})$ Or $(f_{cc,tube}/f_{co})$ ]
Confined concrete core (pitch =50 mm)	62.7	47.3	1.33
Confined concrete core (pitch =75 mm)	53.6	47.3	1.13
Confined concrete inside steel tube ST33.7 (pitch =50 mm)	141	54.2	2.60
Confined concrete inside steel tube ST33.7 (pitch =75 mm)	122	54.2	2.25
Confined concrete inside steel tube ST26.9 (pitch =50 mm)	185	54.2	3.41
Confined concrete inside steel tube ST26.9 (pitch =75 mm)	127	54.2	2.34

Note:

$f_{co}$  represents the unconfined concrete strength.

$f_{cc,core}$  represents the compressive strength of the confined concrete core.

$f_{cc,tube}$  represents the compressive strength of the confined concrete inside the steel tube.

Table 4–Influence of the compressive strength of concrete on the maximum axial load and ductility of columns

Concrete compressive strength, MPa	Maximum axial load of specimens, kN		Ductility of specimens	
	ST33.7H50C*	ST26.9H50C†	ST33.7H50C*	ST26.9H50C†
30	2236	2085	16.0	18.5
40	2370	2150	15.4	17.4
50	2622	2472	14.2	16.6
60	2856	2720	12.9	14.4

\* Yield strength of ST33.7 steel tube was 450 MPa.

† Yield strength of ST26.9 steel tube was 355 MPa.

Table 5—Influence of the tensile strength of steel tube on the maximum axial load and ductility of columns

Tensile strength of steel tube MPa	Maximum axial load of specimens*			Ductility of specimens*	
	ST33.7H50C <sup>†</sup>	ST26.9H50C <sup>‡</sup>	ST33.7H50C <sup>†</sup>	ST33.7H50C <sup>†</sup>	ST26.9H50C <sup>‡</sup>
300	2515	2510	13.8	15.4	
400	2651	2639	13.7	15.3	
500	2782	2760	13.6	15.2	
600	2910	2880	13.5	15.1	

\* Concrete compressive strength of specimens was 57 MPa.

<sup>†</sup> Wall thickness of ST33.7 steel tube was 2 mm.

<sup>‡</sup> Wall thickness of ST26.9 steel tube was 2.6 mm.

**Table 6–Influence of the wall thickness of steel tube on the maximum axial load and ductility of columns**

Wall thickness of steel tube mm	Maximum axial load of specimens*		Ductility of specimens*	
	ST33.7H50C†	ST26.9H50C‡	ST33.7H50C†	ST26.9H50C‡
1.5	2588	2427	13.5	14.6
2.0	2729	2502	13.7	14.8
2.5	2834	2570	13.9	15.1
3.0	2944	2632	14.3	15.5

\* Concrete compressive strength of specimens was 57 MPa.

† Yield strength of ST33.7 steel tube was 450 MPa.

‡ Yield strength of ST26.9 steel tube was 355 MPa.



**Table 7**—Influence of the pitch of steel helices on the maximum axial load and ductility of columns

Pitch of steel helices mm	Maximum axial load of specimens* kN reinforced with		Ductility of specimens* reinforced with	
	ST33.7 steel tube <sup>†</sup>	ST26.9 steel tube <sup>‡</sup>	ST33.7 steel tube <sup>†</sup>	ST26.9 steel tube <sup>‡</sup>
40	2772	2640	14.7	16.7
60	2687	2553	12.8	14.8
80	2660	2450	10.8	12.7
100	2580	2367	9.2	10.0

\* Concrete compressive strength of specimens was 57 MPa.

<sup>†</sup> Yield strength of ST33.7 steel tube was 450 MPa.

<sup>‡</sup> Yield strength of ST26.9 steel tube was 355 MPa.

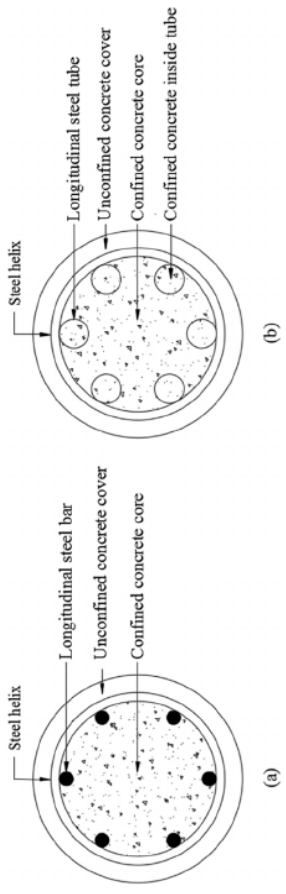
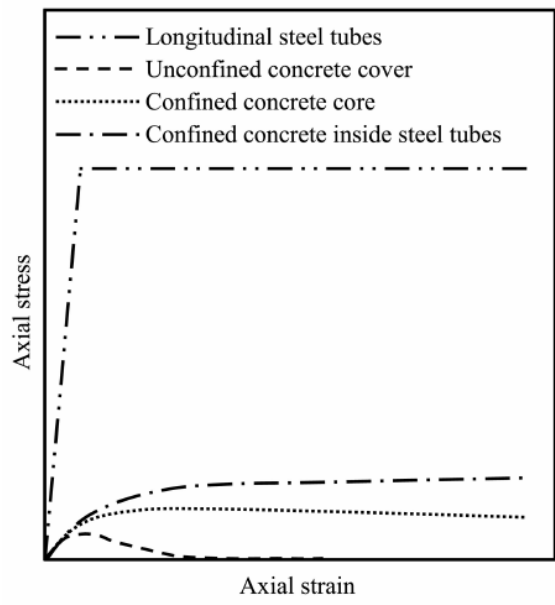
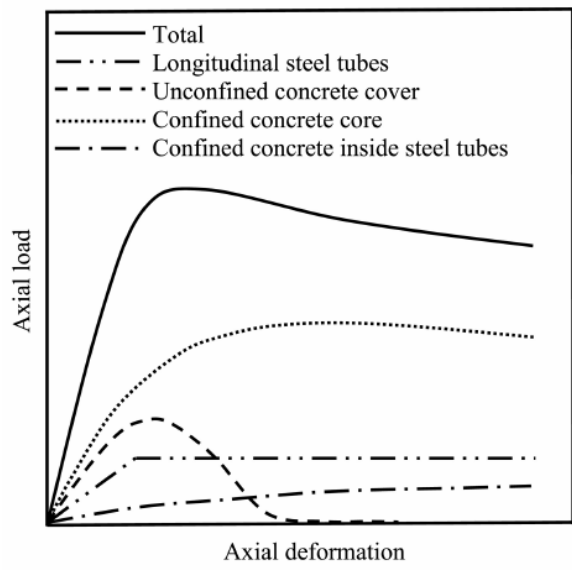


Figure 1



(a)



(b)

Figure 2

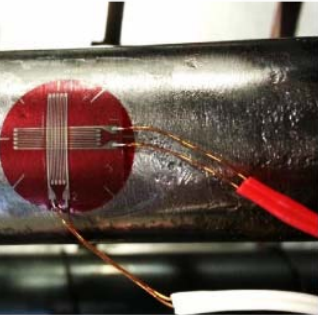




Photo of biaxial two element strain gauges gluing

-  Biaxial two element strain gauges attached to the steel tubes
-  Single element strain gauges attached to the steel helices

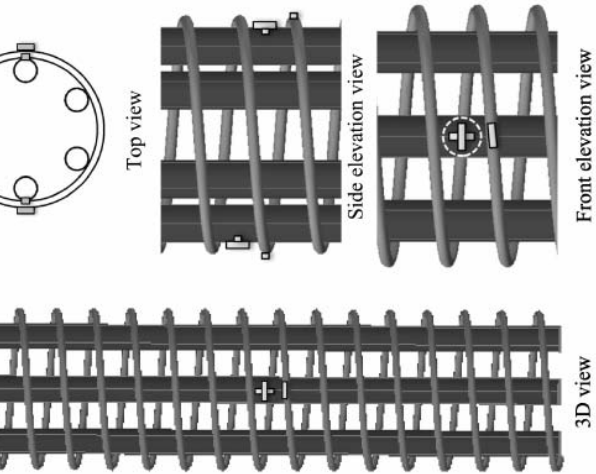


Figure 3

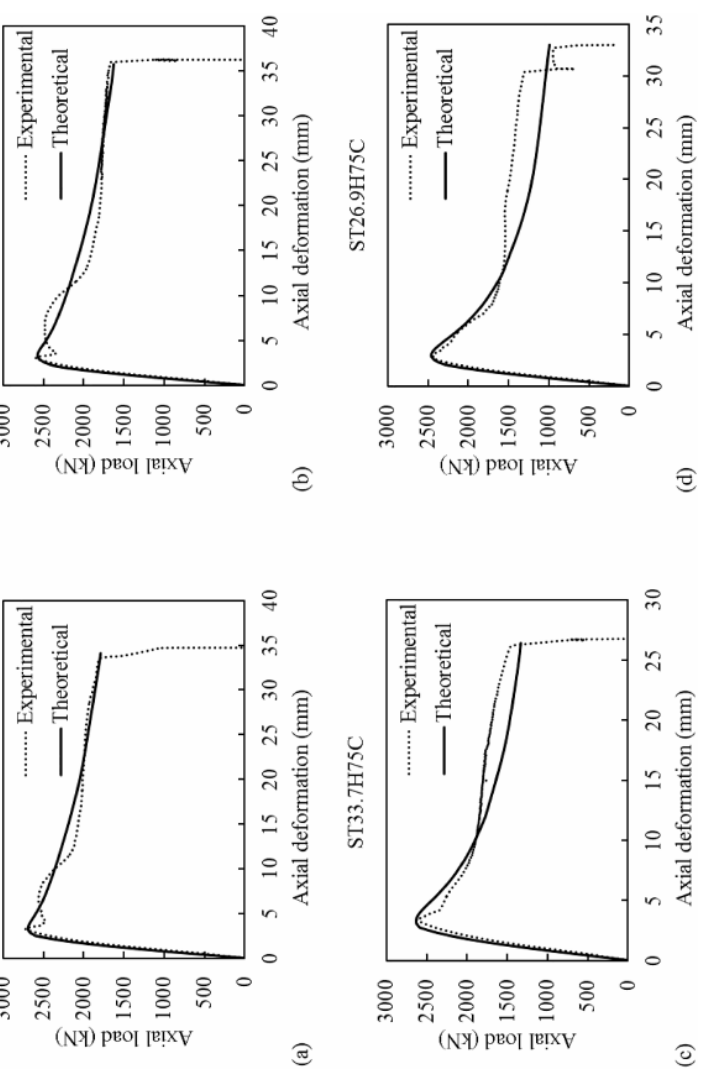


Figure 4

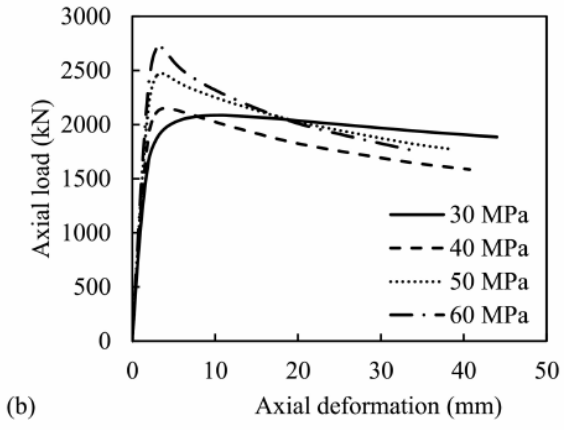
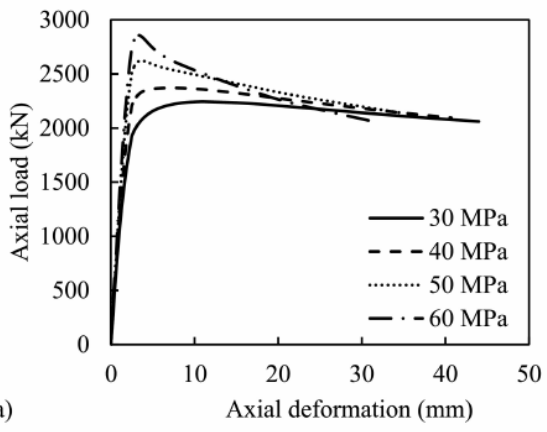


Figure 5

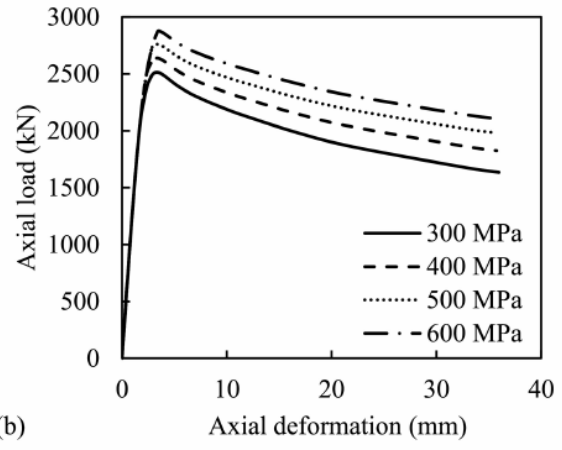
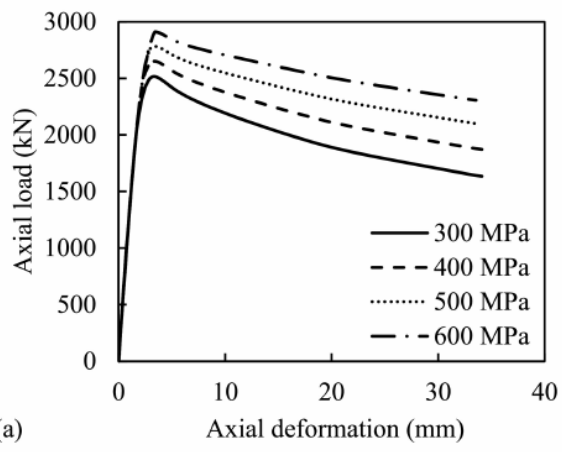


Figure 1

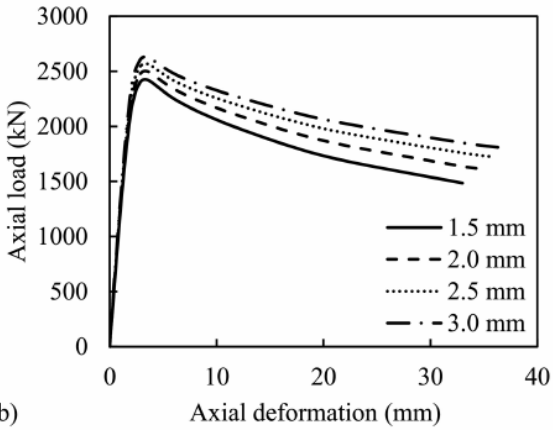
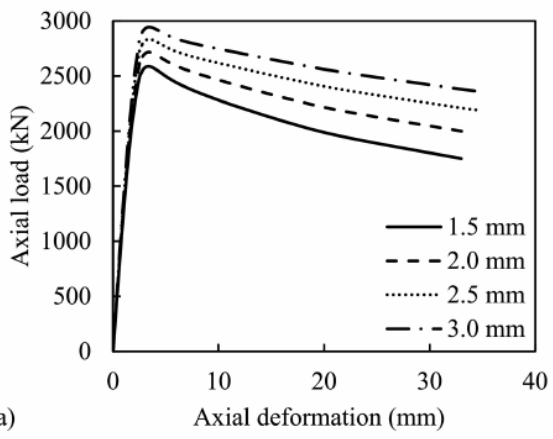


Figure 2



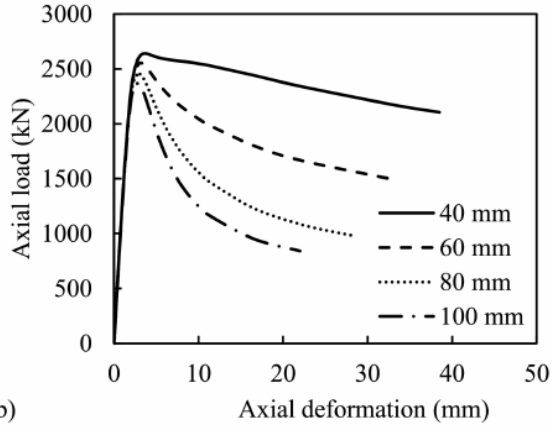
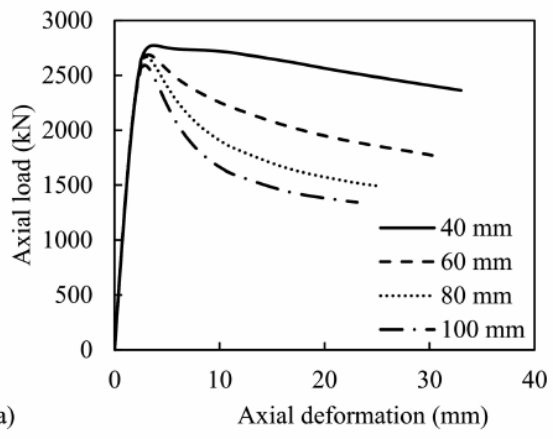


Figure 8